

Structural, magnetic, and ferroelectric properties of $\text{CuFe}_{1-x}\text{Mn}_x\text{O}_2$

K. Hayashi, R. Fukatsu, T. Nozaki, Y. Miyazaki, and T. Kajitani

Department of Applied Physics, Graduate School of Engineering, Tohoku University, Sendai, 980-8579, Japan

(Received 20 July 2012; revised manuscript received 10 December 2012; published 20 February 2013)

We have investigated the structural, magnetic, and ferroelectric properties of Mn-substituted CuFeO_2 , i.e., $\text{CuFe}_{1-x}\text{Mn}_x\text{O}_2$ ($0 \leq x \leq 0.2$). CuFeO_2 is a typical frustrated triangular lattice antiferromagnet due to its Fe^{3+} triangular configuration. Although the lattice constants and atomic bond distances do not change in the range of $0 \leq x \leq 0.2$, structural modulation introduced by the Mn substitution affects the magnetic and dielectric properties. A multiferroic phase, where the antiferromagnetism and ferroelectricity coexist, is found in a narrow range of $0.01 \leq x \leq 0.1$. The origin of the multiferroic characteristics is discussed in terms of the partial release of the spin frustration.

DOI: [10.1103/PhysRevB.87.064418](https://doi.org/10.1103/PhysRevB.87.064418)

PACS number(s): 75.85.+t

I. INTRODUCTION

It is important for basic physics to investigate the relationship between the crystal structure and physical properties of geometrically frustrated triangular lattices. As a model material of the frustrated triangular lattice antiferromagnets, the magnetic properties of CuFeO_2 have been extensively studied due to its layered triangular lattices of Fe^{3+} ions.¹⁻⁵ With decreasing temperature, the CuFeO_2 shows successive magnetic transitions from the paramagnetic (PM) to spin-liquid phase at $T_0 \sim 100$ K, and finally to the four-sublattice antiferromagnetic phase (4SL) at $T_{N1} \sim 10.5$ K. The origin of the spin-liquid phase is the spin frustration inherent in the triangular lattice.⁵ The spin-density wave (SDW) phase coexists within the spin-liquid phase in the temperature range between $T_{N2} \sim 14$ K and T_{N1} . The magnetic transition at T_{N2} is accompanied by the structural transition from a delafossite structure ($R\bar{3}m$) to a monoclinic one ($C2/m$).^{6,7} Recently, CuFeO_2 has received considerable attention due to the simultaneous emergence of antiferromagnetism and ferroelectricity, i.e., the multiferroic phase, by applying a magnetic field^{8,9} or substituting Fe^{3+} for nonmagnetic trivalent ions.¹⁰⁻¹⁴ In the multiferroic phase, structural modulation associated with displacements of the oxygen atoms occurs, which is responsible for the coexistence of complex non-collinear screw-type antiferromagnetic structure and electrical polarization.^{7,15} It is suggested that the structural modulation originates from partial release of the spin frustration.¹⁶ Thus, the appearance of the multiferroic phase should relate to the spin frustration; however, the relationship is not yet fully understood.

In this study, we investigate the structural, magnetic, and dielectric properties of partly Mn-substituted CuFeO_2 . CuFeO_2 belongs to the $R\bar{3}m$ space group with undistorted FeO_6 octahedra above T_{N1} , while CuMnO_2 has a crednerite structure ($C2/m$) with distorted MnO_6 octahedra due to the Jahn-Teller effect.^{17,18} The primary intention of partial Mn^{3+} substitution for Fe^{3+} was to introduce local Jahn-Teller distortions, i.e., structural modulation, in the triangular lattice. In fact, a considerable low thermal conductivity of the partly Mn-substituted CuFeO_2 is ascribed to the structural modulation.¹⁹ Thus, we expect that the introduced structural modulation may affect the magnetic and dielectric properties: The spin frustration is relieved, leading to the multiferroic

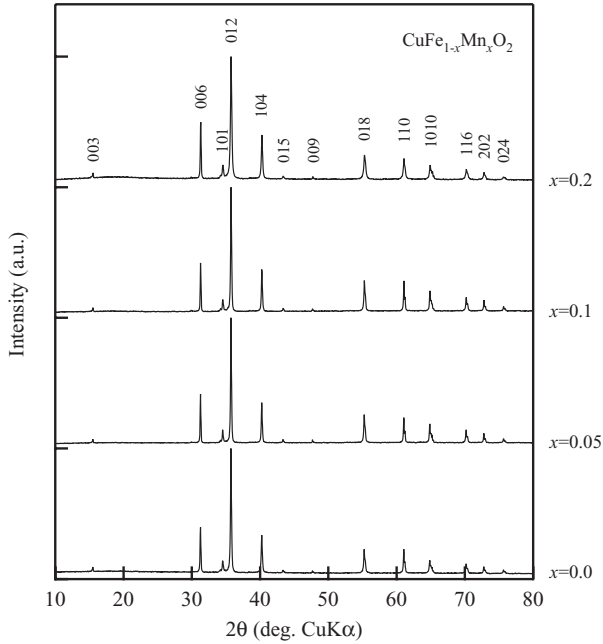
phase. We examine whether the partial Mn substitution might yield the multiferroic phase or not, and discuss the relationship between the multiferroic ordering and spin frustration.

II. EXPERIMENTAL

Polycrystalline samples of $\text{CuFe}_{1-x}\text{Mn}_x\text{O}_2$ ($0 \leq x \leq 0.2$) were prepared by a conventional solid-state reaction method. Starting materials, CuO (Kojundo Chemical Laboratory, 99.9%), Fe_2O_3 (Rare Metallic, 99.9%), and MnO (Kojundo Chemical Laboratory, 99.9%) were mixed, pressed into pellets, and sintered in an Ar gas flow (200 ml/min) for 12 hours. The sintered temperature was varied in proportion to the Mn-substitution content x between 1333 K ($x = 0$) and 1313 K ($x = 0.2$). The crystal structure of the samples was characterized by powder x-ray diffraction (XRD) measurement using a $\text{CuK}\alpha$ radiation source (Rigaku, RAD-X). The XRD peak intensities were analyzed by a Rietveld refinement program, RIETAN 2000.²⁰ The magnetic susceptibility was measured during cooling in the temperature range between 2 and 300 K using a superconducting quantum interference device magnetometer (Quantum Design, MPMS). The dielectric permittivity was measured during heating from 5 to 20 K using a LCR meter (HP, 4284A) at a frequency of 10 kHz. In addition, the electric polarization was measured using a pyroelectric current method. The samples were cooled down to 5 K in a poling field of 400 kV/m. Then, the poling field was removed, and the pyroelectric current was collected upon warming from 5 to 20 K.

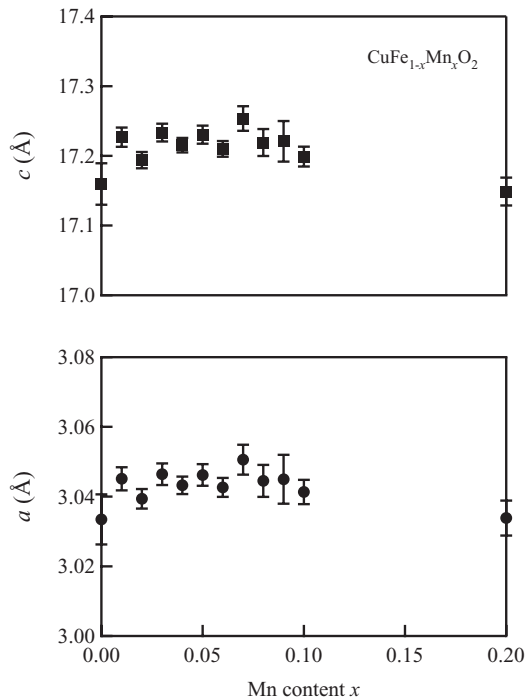
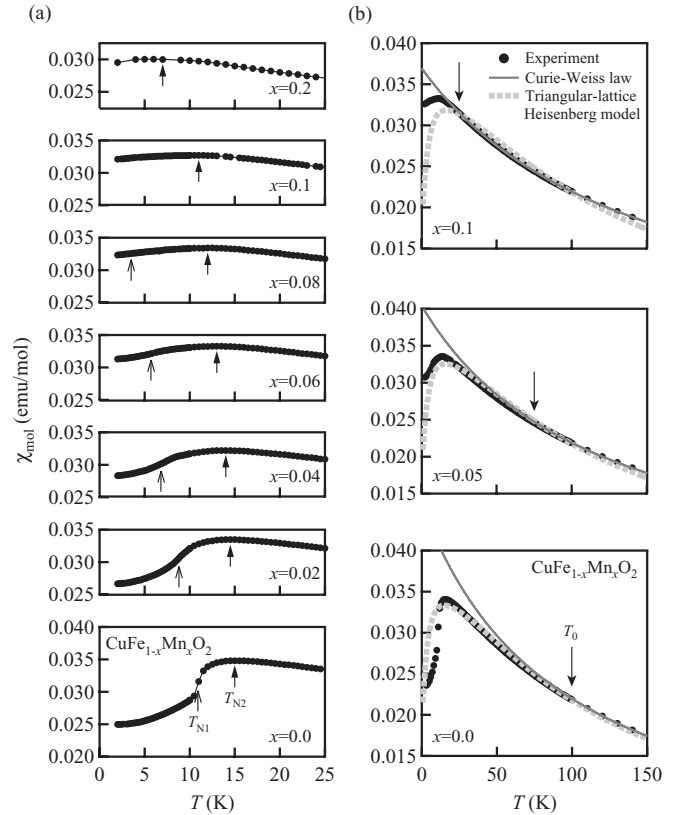
III. RESULTS AND DISCUSSION

Figure 1 shows XRD patterns of $\text{CuFe}_{1-x}\text{Mn}_x\text{O}_2$ ($x = 0, 0.05, 0.1, \text{ and } 0.2$). Due to a higher Ar flow rate in the present study than in the previous study,¹⁹ no impurity phase was detected. Unfortunately, we could not verify the existence of structural modulation from the powder XRD measurement. Note that the XRD patterns showed that the present samples were the delafossite phase in the range of $0 \leq x \leq 0.2$, consistent with the previous study.¹⁹ There was little difference in the XRD peak intensities and peak positions among the samples, indicating that the lattice parameters were almost unchanged as shown in Fig. 2. The lattice parameters a and c exhibited few variations among the samples, which is


 FIG. 1. XRD patterns of $\text{CuFe}_{1-x}\text{Mn}_x\text{O}_2$.

attributed to close ionic radii of Fe^{3+} and Mn^{3+} . Although not shown here, the Cu-O, (Fe/Mn)-O, Cu-Cu, and (Fe/Mn)-(Fe/Mn) interatomic distances were also unchanged. Thus, there is no need to consider the (Fe/Mn)-(Fe/Mn) distance dependence on the exchange interaction, i.e., on the magnetic transition temperatures.

To determine the magnetic transition temperatures, we measured magnetic susceptibility $\chi_{\text{mol}}(T)$ curves of $\text{CuFe}_{1-x}\text{Mn}_x\text{O}_2$ ($0 \leq x \leq 0.2$) as shown in Fig. 3(a). Since


 FIG. 2. Lattice parameters a and c of $\text{CuFe}_{1-x}\text{Mn}_x\text{O}_2$ as a function of Mn content x .

 FIG. 3. Magnetic susceptibility of $\text{CuFe}_{1-x}\text{Mn}_x\text{O}_2$ in (a) narrow and (b) wide temperature ranges. The magnetic transition temperatures T_{N1} , T_{N2} , and T_0 are indicated by arrows.

CuFeO_2 is known to exhibit an anisotropic magnetization parallel and perpendicular to the triangular lattice planes below T_{N2} ,¹² accurate determination of the magnetic transition temperatures from the $\chi_{\text{mol}}(T)$ curves of polycrystalline $\text{CuFe}_{1-x}\text{Mn}_x\text{O}_2$ samples is difficult. With decreasing temperature, the $\chi_{\text{mol}}(T)$ curves were characterized by a broad peak followed by an abrupt decrease. Such characteristics were also reported for the polycrystalline $\text{CuFe}_{1-x}\text{Rh}_x\text{O}_2$.¹⁴ In the literature,¹⁴ the peak and decrease were interpreted as a cascade magnetic transition at T_{N2} and T_{N1} . We adopted this interpretation, and evaluated the peak temperature as T_{N2} and the temperature at the inflection point of the abrupt decrease as T_{N1} . In fact, T_{N1} and T_{N2} evaluated in this way coincided well with those determined from the $\chi_{\text{mol}}(T)$ curves of the CuFeO_2 single crystal.¹² For the samples with $x \geq 0.1$, we could not determine T_{N1} in the measured temperature range above 2 K. As can be seen in Fig. 3(a), T_{N1} and T_{N2} both decreased as a function of the Mn content x . Similar behavior is observed for $\text{CuFe}_{1-x}\text{Rh}_x\text{O}_2$.¹⁴ However, in the cases of $\text{CuFe}_{1-x}\text{Al}_x\text{O}_2$ and $\text{CuFe}_{1-x}\text{Ga}_x\text{O}_2$, only T_{N1} decreases. T_{N2} does not significantly change in spite of the Al or Ga substitution.¹³

Here, we discuss the different tendency of magnetic transition temperatures T_{N1} and T_{N2} among the samples. The change of magnetic transition temperature is caused by three factors: the dilution effect, change of exchange interaction, and partial release of spin frustration due to the structural modulation. The magnetic transition temperature decreases in the presence of dilution effect. The exchange interaction would

increase or decrease the magnetic transition temperature, reflecting the decrease or increase of lattice parameters by the substituent. Since the lattice parameters do not change due to the close ionic radii of Mn^{3+} and Rh^{3+} to that of Fe^{3+} , the exchange interaction is also unchanged by the Mn or Rh substitution. Thus, there is no effect of exchange interaction on the magnetic transition temperature for $\text{CuFe}_{1-x}\text{Mn}_x\text{O}_2$ and $\text{CuFe}_{1-x}\text{Rh}_x\text{O}_2$. On the other hand, the ionic radii of Al^{3+} and Ga^{3+} are smaller than that of Fe^{3+} . In other words, the exchange interaction increases due to the decreasing lattice parameters by the Al or Ga substitution, leading to the increase of magnetic transition temperature. The partial release of spin frustration causes the increase of magnetic transition temperature. Therefore, the almost constant T_{N2} independent of the Al or Ga substitution indicates the existence of these competing three factors. Probably, in the cases of $\text{CuFe}_{1-x}\text{Mn}_x\text{O}_2$ and $\text{CuFe}_{1-x}\text{Rh}_x\text{O}_2$, the dilution effect is superior to the partial release of spin frustration, and hence both T_{N1} and T_{N2} decreased.

To confirm the partial release of spin frustration for $\text{CuFe}_{1-x}\text{Mn}_x\text{O}_2$, we analyzed the $\chi_{\text{mol}}(T)$ curves of $\text{CuFe}_{1-x}\text{Mn}_x\text{O}_2$ ($x = 0, 0.05$, and 0.1) over a wide temperature range [Fig. 3(b)]. The solid curves were fitted by the Curie-Weiss law, i.e., $\chi = C/(T - \theta)$, where C and θ are the Curie constant and Weiss temperature, respectively. The $\chi_{\text{mol}}(T)$ curve of CuFeO_2 can be well fitted from 300 K down to 100 K, while $\chi_{\text{mol}}(T)$ deviated from the Curie-Weiss curve at the temperature lower than 100 K. The evaluated effective magnetic moment and Weiss temperature were $5.82 \mu_B$ and 93 K, respectively, consistent with literature values.^{2,21,22} The deviation from the Curie-Weiss curve corresponds to the magnetic transition from the PM to spin-liquid phases at $T_0 \sim 100$ K.⁵ It is noted that the transition temperature agrees well with the Weiss temperature. The phase transition was also found for $\text{CuFe}_{1-x}\text{Mn}_x\text{O}_2$ ($x = 0.05$ and 0.1). The transition temperature T_0 decreased with increasing x , an indication of a partial release of the spin frustration. A possible reason for the partial release of the spin frustration is the structural modulation introduced by the partial Mn substitution.

Since the spin-liquid phase originates from the frustrated spin configuration in the triangular lattice, we attempted to fit the $\chi_{\text{mol}}(T)$ curve of CuFeO_2 below 100 K using the triangular-lattice Heisenberg model.²³ This model was successful in explaining $\chi_{\text{mol}}(T)$ curves of organic triangular lattice systems, the candidate spin-liquid materials.^{24,25} We adopted the [6/6] Padé approximants for the high-temperature series expansion of triangular-lattice Heisenberg model, $\chi = N_A g^2 \mu_B^2 / (4k_B T) \cdot \sum_n a_n (J/T)^n / (4^{n+1} n!)$, where N_A , g , μ_B , k_B , and J are Avogadro's number, the g factor, a Bohr magneton, the Boltzmann constant, and a nearest neighbor exchange constant, respectively. The integer coefficients a_n used are the literature value.²³ Fitting results are represented by the broken curves in Fig. 3(b). One can see that the $\chi_{\text{mol}}(T)$ curve of CuFeO_2 from 100 K down to T_{N1} as well as above 100 K was finely explained by the triangular-lattice Heisenberg model. This result verifies the above-mentioned strong spin frustration in CuFeO_2 . With increasing the Mn content x , the $\chi_{\text{mol}}(T)$ curves approached the Curie-Weiss curves instead of the triangular-lattice Heisenberg model, evidence that the Mn substitution partially released the spin frustration.

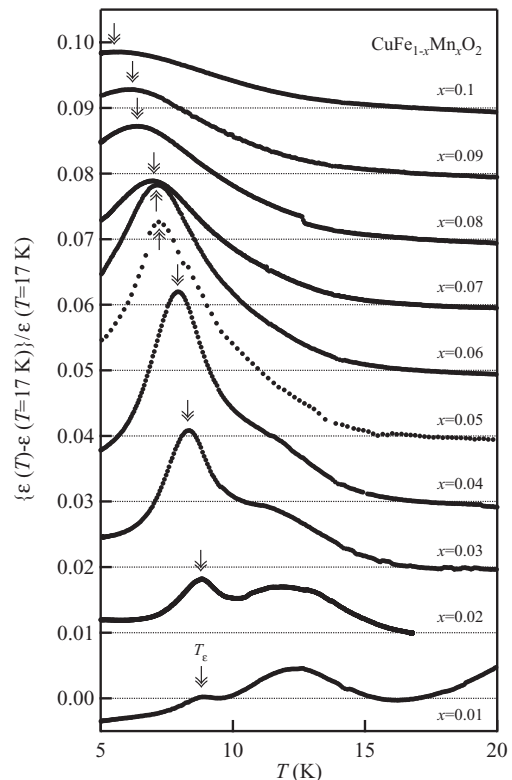


FIG. 4. Relative dielectric permittivity of $\text{CuFe}_{1-x}\text{Mn}_x\text{O}_2$. The peak temperatures T_ϵ , where the ferroelectric transition occurs, are indicated by arrows.

Figure 4 shows the relative dielectric permittivity ϵ curves of $\text{CuFe}_{1-x}\text{Mn}_x\text{O}_2$ ($0.01 \leq x \leq 0.1$). The curves exhibited broad ϵ peaks, which may be attributed to relaxorlike dielectric features due to the microstructural inhomogeneity in the Mn-substituted samples. To investigate the relaxorlike behavior, a frequency dependence of dielectric constants will be measured. Anomalous decrease of ϵ at about 10 K was observed for the samples with $0.01 \leq x \leq 0.04$. This anomaly is related to magnetic hysteresis in the SDW phase where some spin canting takes place.¹⁰ Thus, considering the close relationship between the dielectric and magnetic properties, the broad ϵ peaks may be a result of the broadening of magnetic transition at T_{N1} and T_{N2} for the Mn-substituted samples. For the samples with $x > 0.1$, there was no peak in the $\epsilon(T)$ curves in the temperature range above 5 K (not shown).

To confirm the ferroelectric feature, we measured the temperature dependent electric polarization $P(T)$ of $\text{CuFe}_{1-x}\text{Mn}_x\text{O}_2$. The $\epsilon(T)$ and $P(T)$ curves of the sample with $x = 0.02$ are shown in Figs. 5(a) and 5(b), respectively. It is pointed out that the electric polarization exhibited an increase at 9 K, which is quite close to the ϵ peak temperature T_ϵ of 8.8 K. The corresponding ϵ peak was the one located below 10 K. Since the electric polarization was reversed by applying an inverse poling field as shown in Fig. 5(b), we conclude that all samples with $0.01 \leq x \leq 0.1$ exhibited the ferroelectric transition at T_ϵ . The variation of T_ϵ as a function of x is exhibited in Fig. 4: T_ϵ decreased monotonically with increasing x . In addition, the maximum electric

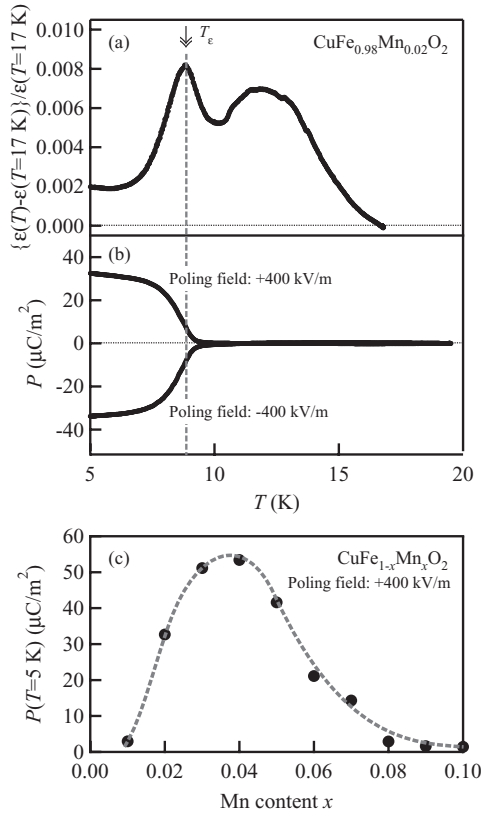


FIG. 5. (a) Relative dielectric permittivity and (b) electric polarization of $\text{CuFe}_{0.98}\text{Mn}_{0.02}\text{O}_2$. (c) Electric polarization at 5 K of $\text{CuFe}_{1-x}\text{Mn}_x\text{O}_2$ as a function of Mn content x .

polarization recorded in the present study was $53\ \mu\text{C}/\text{m}^2$ for the sample with $x = 0.04$ as shown in Fig. 5(c). We cannot simply compare the maximum electric polarization to other multiferroic materials because the $\text{CuFe}_{1-x}\text{Mn}_x\text{O}_2$ was polycrystal and its electric polarization was not saturated in the poling field of $400\text{ kV}/\text{m}$. Reported materials are, for example, $\text{CuFe}_{0.98}\text{Al}_{0.02}\text{O}_2$ single crystal ($35\ \mu\text{C}/\text{m}^2$),¹⁰ $\text{CuFe}_{0.963}\text{Ga}_{0.037}\text{O}_2$ single crystal ($\sim 250\ \mu\text{C}/\text{m}^2$),¹² polycrystalline $\text{CuFe}_{0.92}\text{Rh}_{0.08}\text{O}_2$ ($110\ \mu\text{C}/\text{m}^2$),¹⁴ and TbMnO_3 single crystal ($800\ \mu\text{C}/\text{m}^2$).²⁶ In comparison, the electric polarization of $\text{CuFe}_{1-x}\text{Mn}_x\text{O}_2$ seems to be small. There is a possibility that the small electric polarization is caused by the structural modulation due to partial Mn substitution. To discuss the sample dependency, a saturated electric polarization of $\text{CuFe}_{1-x}\text{Mn}_x\text{O}_2$ single crystal is needed.

In Fig. 6, we illustrate the magnetic and electric phase diagram of $\text{CuFe}_{1-x}\text{Mn}_x\text{O}_2$ ($0 \leq x \leq 0.2$). T_{N1} almost coincided with T_e . Thus, we may conclude that, at least, the red region in the phase diagram is the multiferroic phase. Considering the x dependence of T_0 , the spin-liquid phase would disappear just above $x = 0.1$. In other words, there is a possibility that the spin frustration is completely relieved just above $x = 0.1$. If the appearance of the multiferroic phase strongly couples with partial release of the spin frustration, the multiferroic phase is expected to exist only in the range of $0 < x \leq 0.1$. We will examine this assumption from the magnetic susceptibility, dielectric permittivity, and electric polarization measurements

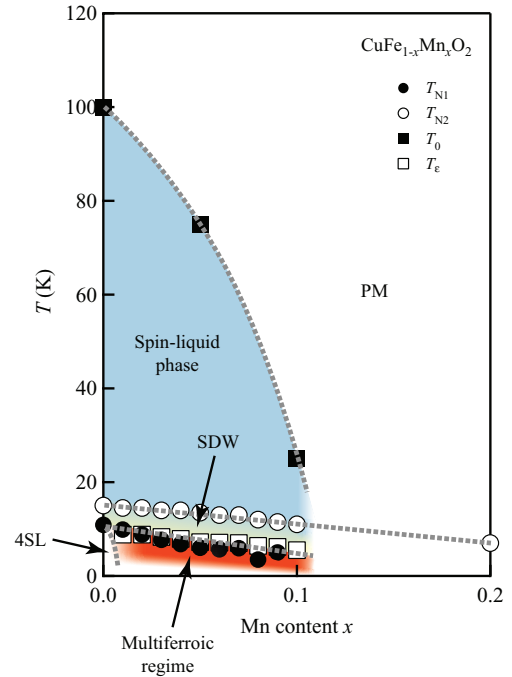


FIG. 6. (Color online) Magnetic and electric phase diagram of $\text{CuFe}_{1-x}\text{Mn}_x\text{O}_2$.

at lower temperatures. Additionally, the release of the spin frustration will be investigated by the quasielastic neutron scattering measurement.²⁷ These measurements enable us to understand the role of spin frustration on the appearance of multiferroic phase further.

IV. CONCLUSION

In this study, we investigated the structural, magnetic, and ferroelectric properties of $\text{CuFe}_{1-x}\text{Mn}_x\text{O}_2$ ($0 \leq x \leq 0.2$). The structure of $\text{CuFe}_{1-x}\text{Mn}_x\text{O}_2$ was delafossite phase for the studied x range, and no distinct change was found in the structural parameters such as the lattice constants and interatomic distances among the samples. The antiferromagnetic phase transition temperatures T_{N1} and T_{N2} decreased with increasing x . The spin-liquid phase transition temperature T_0 also decreased with increasing x , indicating partial release of the spin frustration. Furthermore, we found a ferroelectric phase between $x = 0.01$ and $x = 0.1$ whose transition temperature T_e was almost equal to T_{N1} . Thus, we conclude that a multiferroic phase exists below T_{N1} . These results suggest a close relationship between the multiferroic phase and the partial release of spin frustration.

ACKNOWLEDGMENTS

This work was partly supported by Grants-in-Aid for Scientific Research from the Ministry of Education, Culture, Sports, Science, and Technology of Japan. We thank T. Arima and N. Abe for their help measuring the dielectric permittivity and electric polarization.

- ¹S. Mitsuda, H. Yoshizawa, N. Yaguchi, and M. Mekata, *J. Phys. Soc. Jpn.* **60**, 1885 (1991).
- ²M. Mekata, N. Yaguchi, T. Takagi, T. Sugino, S. Mitsuda, H. Yoshizawa, N. Hosoi, and T. Shinjo, *J. Phys. Soc. Jpn.* **62**, 4474 (1993).
- ³S. Mitsuda, N. Kasahara, T. Uno, and M. Mase, *J. Phys. Soc. Jpn.* **67**, 4026 (1998).
- ⁴N. Terada, T. Kawasaki, S. Mitsuda, H. Kimura, and Y. Noda, *J. Phys. Soc. Jpn.* **74**, 1561 (2005).
- ⁵K. Hayashi, T. Nozaki, R. Fukatsu, Y. Miyazaki, and T. Kajitani, *Phys. Rev. B* **80**, 144413 (2009).
- ⁶R. D. Shannon, C. T. Prewitt, and D. B. Rogers, *Inorg. Chem.* **10**, 719 (1971).
- ⁷F. Ye, Y. Ren, Q. Huang, J. A. Fernandez-Baca, Pengcheng Dai, J. W. Lynn, and T. Kimura, *Phys. Rev. B* **73**, 220404 (2006).
- ⁸T. Kimura, J. C. Lashley, and A. P. Ramirez, *Phys. Rev. B* **73**, 220401(R) (2006).
- ⁹S. Seki, H. Murakawa, Y. Onose, and Y. Tokura, *Phys. Rev. Lett.* **103**, 237601 (2009).
- ¹⁰S. Seki, Y. Yamasaki, Y. Shiomi, S. Iguchi, Y. Onose, and Y. Tokura, *Phys. Rev. B* **75**, 100403(R) (2007).
- ¹¹S. Kanetsuki, S. Mitsuda, T. Nakajima, D. Anazawa, H. A. Katori, and K. Prokes, *J. Phys.: Condens. Matter* **19**, 145244 (2007).
- ¹²N. Terada, T. Nakajima, S. Mitsuda, H. Kitazawa, K. Kaneko, and N. Metoki, *Phys. Rev. B* **78**, 014101 (2008).
- ¹³N. Terada, T. Nakajima, S. Mitsuda, and H. Kitazawa, *J. Phys.: Conf. Ser.* **145**, 012071 (2009).
- ¹⁴E. Pachould, C. Martina, B. Kundys, C. Simon, and A. Maignan, *J. Solid State Chem.* **183**, 344 (2009).
- ¹⁵J. T. Haraldsen, F. Ye, R. S. Fishman, J. A. Fernandez-Baca, Y. Yamaguchi, K. Kimura, and T. Kimura, *Phys. Rev. B* **82**, 020404(R) (2010).
- ¹⁶T. Nakajima, S. Mitsuda, J. T. Haraldsen, R. S. Fishman, T. Hong, N. Terada, and Y. Uwatoko, *Phys. Rev. B* **85**, 144405 (2012).
- ¹⁷I. D. Kondrashev, *Sov. Phys. Crystallogr.* **3**, 703 (1959).
- ¹⁸M. Trari, J. Töpfer, P. Dordor, J. C. Grenier, M. Pouchard, and J. P. Doumerc, *J. Solid State Chem.* **178**, 2751 (2005).
- ¹⁹T. Nozaki, K. Hayashi, and T. Kajitani, *J. Electron. Mater.* **39**, 1798 (2010).
- ²⁰F. Izumi and T. Ikeda, *Mater. Sci. Forum* **321–324**, 198 (2000).
- ²¹O. A. Petrenko, M. R. Lees, G. Balakrishnan, S. de Brion, and G. Chouteau, *J. Phys.: Condens. Matter* **17**, 2741 (2005).
- ²²J.-P. Doumerc, A. Wichainchai, A. Ammar, M. Pouchard, and P. Hagenmuller, *Mater. Res. Bull.* **21**, 745 (1986).
- ²³N. Elstner, R. R. P. Singh, and A. P. Young, *Phys. Rev. Lett.* **71**, 1629 (1993).
- ²⁴M. Tamura and R. Kato, *J. Phys.: Condens. Matter* **14**, L729 (2002).
- ²⁵Y. Shimizu, K. Miyagawa, K. Kanoda, M. Maesato, and G. Saito, *Phys. Rev. Lett.* **91**, 107001 (2003).
- ²⁶T. Kimura, T. Goto, H. Shintani, K. Ishizaka, T. Arima, and Y. Tokura, *Nature (London)* **426**, 55 (2003).
- ²⁷K. Hayashi, R. Fukatsu, T. Nozaki, Y. Miyazaki, and T. Kajitani (unpublished).